Active Mechatronic Interface for Haptic Perception Studies with Functional Magnetic Resonance Imaging: Compatibility and Design Criteria

R Gassert[1], N Vanello[2,3], D Chapuis[1], V Hartwig[4], E Scilingo[4], A Bicchi[4], L Landini[5,3], E Burdet[6], and H Bleuler[1]

[1]Laboratory of Robotic Systems, Ecole Polytechnique Fédérale de Lausanne (EPFL), Switzerland

Email: r.gassert@ieee.org   http://mrrobotics.epfl.ch

[2]Department of Electrical Systems and Automation, Faculty of Engineering, Univ. of Pisa, Italy

[3]MRI Lab, IFC CNR, Pisa, Italy

[4]Interdepartmental Center E. Piaggio, Faculty of Engineering, Univ. of Pisa, Italy

[5]Department of Information Engineering, Faculty of Engineering, Univ. of Pisa, Italy

[6]Department of Bioengineering, Imperial College London, UK; e.burdet@imperial.ac.uk

Abstract— **Functional brain exploration methodologies such as functional magnetic resonance imaging (fMRI) are critical tools to study perceptual and cognitive processes. In order to develop complex and well-controlled fMRI paradigms, researchers are interested in using active interfaces with electrically powered actuators and sensors. Due to the particularity of the MR environment, safety and compatibility criteria have to be strictly followed to avoid risks to the subject under test, the operators or the environment, as well as to prevent artifacts in the images. This paper describes the design of an fMRI compatible mechatronic interface based on MR compatibility tests of materials and actuators. In particular, a statistical test is introduced to evaluate the presence of artifacts in the image sequences that could negatively affect the fMRI studies. The device with two degrees of freedom, allowing one translation with position-feedback along a horizontal axis and one rotation about a vertical axis linked to the translation, was realized to investigate the brain mechanisms of dynamic tactile perception tasks. It can be used to move and orient various objects below the finger for controlled tactile stimulation. The MR compatibility of the complete interface is shown using the statistical test as well as a functional study with a human subject.**
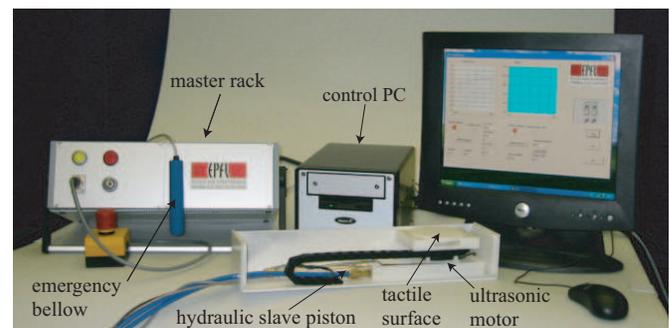
Fig. 1. MR compatible interface to investigate the brain mechanisms of tactile perception. The slave module, shown in the front, contains an active rotary degree of freedom (ultrasonic motor) linked to a translatory degree of freedom (brass hydraulic piston).

I. INTRODUCTION

The investigation of brain function with functional magnetic resonance imaging (fMRI) involves increasingly complex experimental paradigms with randomization of stimuli and parametric design, all under controlled conditions. This requires dedicated mechatronic devices which can precisely control stimuli parameters and measure onset and duration of interaction with the subject. The design of devices to work within an MR environment has to fulfill severe safety and compatibility criteria. Moreover, the scanning sequences used for fMRI studies (gradient-echo echo planar) are very sensitive to changes in static magnetic field homogeneity, varying magnetic fields originating from electrical equipment located in the scanner bore or within the scanner room.

Therefore, design and testing phases of the dedicated devices are crucial to avoid complications. Interaction phenomena between primary components of the MR environment and mechatronic devices have to be considered carefully. A critical issue is related to the effects of strong attracting forces induced by the MR system's static magnetic fields on ferromagnetic objects. The strength of the magnetic field drops off rapidly with increasing distance from the magnet, producing a large spatial gradient which accelerates ferromagnetic objects introduced into the field [1]. Conductors placed near the imaging region can cause image artifacts and distortions, as they may produce local field inhomogeneities [2] which are related to the susceptibility difference between the tissue to be imaged and the metallic object.

Artifacts may also originate from the interaction between conductive materials and time-varying electromagnetic fields, such as gradient and radiofrequency (RF) pulses. These induce eddy currents in conductive materials, which produce a significant local artifact resulting from perturbations of the transmitting and receiving sensitivities of the RF coil. Such fields can also be created by currents running through

electrical equipment placed in the scanner room. The choice of materials that can be used to build dedicated devices for MRI systems is based on magnetic susceptibility: generally, materials with high magnetic susceptibility are considered to be incompatible with MRI and should not be brought near the scanner. The Food and Drug Administration (FDA) [3] provides a useful classification of MR compatibility that can be used for experimental protocols to evaluate compatibility. An "MR compatible" device, when used in the MR environment, must be MR safe and neither significantly affect the quality of the diagnostic information nor be sensitive to the operating MR device.

This paper presents an fMRI compatible mechatronic interface, which was designed based on the reported results of compatibility tests performed with several non-ferromagnetic materials and electric motors. These tests provided an evaluation of MR compatibility issues and significantly contributed to the design of the device, which was developed to investigate the brain mechanisms of tactile perception. This novel interface has two actuated degrees of freedom allowing one translation along a horizontal axis as well as one rotation about a vertical axis linked to the translation. It can be used to move and orient various objects below the finger.

Two different kinds of actuators are used in this interface. An electric DC actuator placed outside the MR room and providing power at a location close to the scanner over a hydrostatic transmission [4] is used to move the stimulation object back and forth below the finger of the subject. An MR compatible force sensor [5] can be incorporated into the linear degree of freedom (DOF) to allow measuring the interaction force with the subject, and to perform force-feedback on this DOF [4]. An ultrasonic motor is used to control the orientation of the stimulation object, which can be changed during the functional imaging (e.g. to investigate orientation-dependent brain activity).

In contrast to the power provided by the hydrostatic transmission, which has been shown to be compatible with fMRI [4], the ultrasonic actuator placed inside the scanner room may affect the imaging as it is powered over electric cables. Furthermore, the imaging could be disturbed not only by the interaction of cables and the RF pulses from the scanner, but also by spurious currents injected in the cables by other equipment located in the control room (such as the PWM controller of the DC motor). Therefore, the MR compatibility of the interface and its components had to be analyzed thoroughly.

A statistical test on image sequences between different experimental conditions was introduced to evaluate changes in signal-to-noise ratio (SNR) values and time domain standard deviations. These tests were performed both during the design phase to determine the compatibility of the individual components and to test the final prototype. Finally, a neural activity map from a finger tapping experiment, performed while the device was running, was estimated. This map was compared with the results from the same task performed without any device in the scanner room.

II. MR COMPATIBILITY TESTS OF MATERIALS AND ACTUATORS

A. Method

Two non-ferromagnetic metals and two types of actuators were examined during MR image acquisition. Cylindrical hollow tubes from aluminium and brass were tested. The effect of the tubes on the images when they were placed at the entrance of the scanner bore was evaluated in two different operating conditions: when they were still, or moved by an operator using a wooden broomstick.

Two types of servo motors were evaluated: a DC motor (RE 40, Maxon Motor, Switzerland) and an ultrasonic motor (USR60-E3N, Shinsei Corp., Japan) [6]. As the DC motor contains ferromagnetic materials and permanent magnets, it is attracted by the static magnetic field and is thus potentially dangerous. Compatibility tests also showed that such an actuator could, if not properly shielded, disturb the imaging even if placed approximately three meters away from the isocenter of the scanner. Therefore, the DC motor will only be used outside the scanner room. The ultrasonic motor, however, is made of non-ferromagnetic materials and is safe to be placed inside the scanner.

For the desired application, the ultrasonic motor located at the output of the device will have to control the output angle in function of the position of the translational degree of freedom. We therefore investigated the MR compatibility of a linear potentiometer connected to a shielded cable that could be used as simple and low-cost position sensor along this DOF. Two different potentiometers were tested: one with a carbon conductive element (potentiometer A) and one with a plastic conductive element and gold wipers (potentiometer B). RF filters were placed at the level where the cable passes through the penetration panel.

In all experiments, a spherical phantom of copper sulphate ($CuSO_4$) solution was scanned using a GE-EPI (gradient-echo echo planar imaging) sequence with the following parameters: TE/TR $40/3000$ ms, bandwidth 62.5 kHz, FOV 24 cm, resolution 64×64 pixels, flip angle $90°$, twenty 5 mm thick axial slices, and 25 time frames. The first five time frames were discarded to ensure that the magnetization reached the equilibrium. All experiments were performed with a 1.5 T General Electric Signa CV\i scanner.

The SNR, corrected for different statistics of the noise in the phantom compared to the background [7], was defined as:

$$SNR = \frac{P_{center}}{(1.53/4)\sum_{i=1}^{4} SD_i} \qquad (1)$$

where P_{center} is the mean value of a 10×10 voxel area at the center of the image, and SD_i is the mean standard deviation of the ith of four 5×5 voxel areas in the corners of the image. This operation was repeated for each image so that 20 SNR estimates were computed for each sequence.

While SNR is estimated to look for degradation of image quality, another measure is required to examine whether the deviation of the signal of a voxel over time is affected by

materials or electrical equipment used during the imaging. For this purpose, we computed the standard deviation (SD) of the image intensity time-course for each image sequence from a 15×15 voxel region of interest (ROI) located in the center of the phantom, resulting in 225 SD values for each image sequence.

The test aimed at evaluating the differences between the mean values of the above parameters (SNR and SD), estimated from images with only the phantom (reference images or baselines) and the phantom along with the material, actuator or mechatronic device to be tested. Given the means of the two populations for the parameter of interest, μ_1 and μ_2, the hypothesis to be tested is the null hypothesis H0: $\mu_1 = \mu_2$, indicating that the presence of the component does not influence the imaging. In our case, we will use the alternative bidirectional hypothesis H1: $\mu_1 \neq \mu_2$, indicating that the components significantly disturb the imaging.

An unpaired t test was used to detect differences between SNR means of two sets of images. The t value is positive if the mean of the first condition is larger than the second one and negative if it is smaller. If the estimated absolute t value is larger than the critical one, it can be inferred that the difference between the means of the two groups is statistically significant and that the images are significantly affected by artifacts. The degrees of freedom for the t test on SNR are calculated as $n_1 + n_2 - 2$, where n_1 and n_2 are the number of SNR estimates for each image sequence. Choosing a 5% significance level with 38 degrees of freedom leads to a critical t value of 2.024.

A z test was used to detect significant differences in the means of time domain standard deviations estimated from two EPI image sequences, as n_1 and n_2 are sufficiently large in this case and z values can thus be assumed to be normally distributed. The absolute critical value for the bidirectional alternative hypothesis corresponding to a 5% significance level is $z_c = 1.96$.

B. Results

The results of the MR compatibility tests with the different materials and actuators are shown in Table I. As system instabilities can cause the SNR to vary strongly over time [8], several baseline sequences were acquired at different times in the same session in order to examine whether they were affected by significant differences. Having verified that there was no relevant change among the baseline sequences, one baseline was randomly selected as reference.

Brass and aluminum pipes were tested when positioned at the entrance of the scanner bore (experiments #4 and #6, Table I) and moving along the z-axis, aligned with the patient bed and the static magnetic field (experiments #5 and #7). The results show no significant difference between the sequences with materials and the baseline sequences.

The ultrasonic motor was found to be compatible both in off and working conditions, even when loaded (maximum driving current about 0.4 A at 130 V_{rms}).

The image sequence acquired with potentiometer A showed significant differences to the baseline images, while linear potentiometer B did not produce significant changes in the parameters we tested.

From these results we conclude that brass and aluminium pipes can be used for MRI/fMRI compatible devices located in the hand region (entry of the scanner bore) or further away, both for static and moving components. The ultrasonic motor allows good position control and can be employed to orient the output of the device. The translation can be actuated using a hydrostatic transmission as presented in [4], which has a linear output, can generate high force, and can be extended for force-feedback during fMRI by adding a force sensor. Potentiometer B can provide position feedback of the translational movement. As all the power cables pass the Faraday cage surrounding the scanner room through the waveguides, RF filters were added to remove RF noise that may be picked up by the cables from outside the scanner room (e.g. from a PWM amplifier) or from the scanner and create artifacts in the images.

TABLE I

Results of the statistical tests on the means of SNR and t SD, respectively, between reference images (phantom only) and images acquired with the components to be tested. t values for SNR and z values for time domain standard deviation are shown. SNR t critical value = 2.024, SD z critical value = 1.96. For higher values, we conclude that a component significantly disturbs the MR imaging and cannot be used at the given location.

	Slice #5		Slice #10		Slice #20	
Experiment #	t SNR	z SD	t SNR	z SD	t SNR	z SD
1 Test between baseline images	0.05	−1.28	1.39	−0.07	−1.41	−0.24
2 Ultrasonic Motor: turned off at bore entrance	−0.15	1.86	−0.73	0.2	−0.91	0.25
3 Ultrasonic Motor: on condition at bore entrance	−0.03	0.1	−1.21	0.75	0.42	−0.13
4 Brass tube fixed at bore entrance	0.11	−0.86	−0.35	−0.07	0.48	−1
5 Brass tube moving along z inside the scanner	0.18	−1.17	−0.68	0.87	−0.03	0.36
6 Aluminium tube fixed at bore entrance	−1.96	−0.16	−1.72	−0.6	0.72	1.07
7 Aluminium tube moving along z inside the scanner	−1.69	−0.3	−0.23	−1.86	−1.18	0.96
8 Shielded cable with potentiometer A and 0.25 mA electric current	−2.07	−4.88	5.16	−3.49	6.3	−3.15
9 Shielded cable with potentiometer B and 0.25 mA electric current	−1.1	−1.92	−1	−0.56	−1.3	−0.98

III. DESIGN OF THE INTERFACE

Based on the results of the above compatibility tests we were able to choose the materials and actuators with the best properties for the selected application that will guarantee MR safety and compatibility in the desired working region. These results influenced the design of a mechatronic device for the controlled presentation of tactile stimuli during fMRI.

In contrast to the interface of [4], [9], this new interface uses electrically powered components inside the MR room to generate mechanical motion and measure the position of the linear degree of motion over a sensor.

The MR compatibility tests in an early stage of development allowed us to establish the following design guidelines:

- Non-ferromagnetic metals can be used in the hand region, both for fixed and moving components. For our application, this has the advantage that friction can be reduced in the hydrostatic transmission and smaller components can be realized with respect to components made from polymers.
- The ultrasonic motor is fMRI compatible and can be well controlled in position. It is used to power the rotary degree of freedom of the device.
- A linear potentiometer with plastic conductive elements and gold wipers is a low-cost alternative to measure the position of the slave piston.
- The electric cabling required for the ultrasonic motor and the linear potentiometer acts as an antenna and can pick up RF signals emitted by the MR scanner or other equipment like the PWM amplifier of the DC motor and disturb the imaging. Therefore, these components can only be used in specific locations (e.g. at a minimum distance from the scanner bore), and require shielding, power and signal filtering as well as MR compatibility testing.

On the realized interface, a master-slave system with hydrostatic transmission is used to actuate the linear degree of freedom. The transmission uses double-acting, single-ended pistons made from brass. The slave cylinder can be disconnected from the master cylinder to allow easy installation of the interface within the MR facility. The transmission length is eight meters. The master hydraulic cylinder is actuated by a DC torque motor (Fig. 4) over a differential belt and pulley system.

The rotary degree of freedom is actuated by the ultrasonic motor evaluated previously. The slave system is integrated into a glass fiber box, as shown in Fig. 3.

The master DC torque motor is equipped with a commercial quadrature encoder with 20000 imp/rev. The displacement of the slave piston is measured using a linear potentiometer mechanically linked to the slave piston. The ultrasonic motor is also equipped with a quadrature encoder.

The interface is controlled by a commercial PC running Windows and developed control software created with LabWindows from National Instruments. The hardware is controlled over a Multifunction DAQ card from National Instruments connected to a custom designed interface/security PCB. This PCB holds the interfacing electronics that convert the encoder signals to the requirements of the acquisition card as well as the logic circuits that monitor the security hardware.

Power sources, safety hardware and the interface/security PCB are contained in a master rack shown in Fig. 1A. The interface is controlled at 500 Hz, which is sufficient for the used hydrostatic transmission [10].
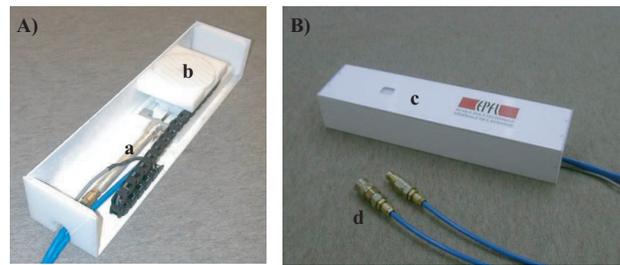

Fig. 2. The slave module. A) Without cover, showing the slave hydraulic piston (a) and the tactile pad (b). The ultrasonic motor is located beneath the tactile pad. B) The closed module showing the touch-pad (c) and the disconnectable (d) hydrostatic transmission.
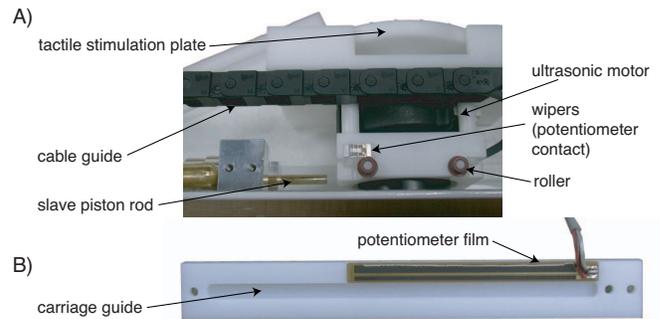

Fig. 3. A) Close-up view of the carriage in the slave module. The carriage is actuated by the slave piston and held by two lateral guides. The right guide (B) also holds the potentiometer film.

As this interface will be used by a human subject within an MR environment, safety is a crucial factor. The developed interface presents the following safety features [4]:

- A master emergency button (which can be disconnected from the master rack) for the experiment supervisor to cut power to the DC and ultrasonic motors.
- A security bellow for the subject in the MR scanner to disable the DC and ultrasonic motors and avert the experiment supervisor over a pneumatic hose and switch shown in Fig. 1.
- Electrical end-of-travel switches on the master actuator to disable the DC torque motor if the master piston moves past the desired position (these positions can be adjusted by moving the switches).
- Mechanical end-of-travel limitations (intrinsic property of the hydraulic cylinder).
- Software security routines which monitor position and speed of the DC and ultrasonic motors.
- A master enable-button located on the master rack to disable the DC and ultrasonic motor.

If any of these security features is activated, the green enable-button on the master rack is deactivated and a red security lamp lights up to alert the experiment supervisor.
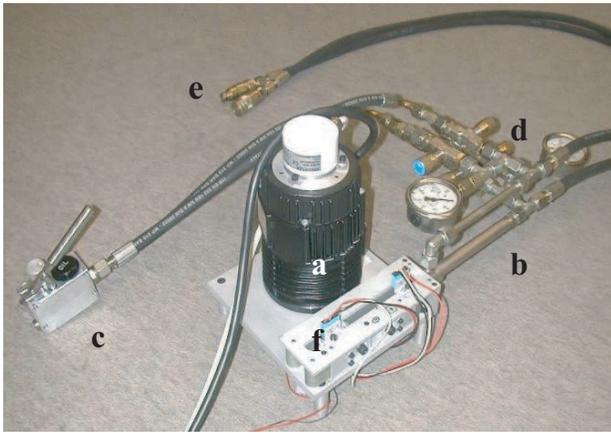
Fig. 4. The master actuator: DC torque motor (a), master hydraulic cylinder (b), hydraulic pump (c) and circuitry (d) as well as disconnectable hydrostatic transmission (e) and security switches (f).

IV. MR Compatibility Tests of the Interface

A. Method

1) Phantom Tests: MR compatibility of the haptic interface was tested with a phantom placed within the scanner. The slave module was placed at bore entrance on one side of the patient bed, the position planned for experiments with a subject. The master actuator and the master control rack were placed outside the scanner room. Both the DC motor in the master actuator module and the ultrasonic motor were running.

2) Functional Study with a Subject: Although the device proposed here is dedicated for passive dynamic tactile stimuli, a finger tapping experiment – a common test of motor activity – was performed on a 25-year-old right-handed subject. This choice is justified by the need of a reference paradigm in neural activation, also when the device is off. The subject gave informed consent for the test. One spoiled grass 3D T1 weighted anatomical image was acquired. The functional scans were gradient echo planar images with $TR = 3$ *s*, $TE = 40$ *ms*, $FA = 90°$ and 62.5 *kHz* bandwidth. Twenty axial slices covering the whole brain where acquired with a slice thickness of 5 *m*, 24 *cm* FOV, and an in-plane 64×64 spatial resolution. The number of time frames was 25. The subject's head was restrained with foam in order to minimize head movements. In all the scans, the subject performed a simple finger tapping sequence with the fingers of his right hand. The task was a simple block design paradigm alternating between 15 *s on* and 15 *s off* conditions. This task was performed without any equipment in the scanner room (reference images), and with the haptic interface running in the scanner room.

The activation maps were obtained by means of a regression analysis [11]: the regressor of interest was obtained convolving a square wave describing the paradigm with a model for the hemodynamic response function given by $h(t) = kt^{8.6}e^{-t/0.547}$ [12]. A mean value and a linear ramp were used in the model as regressors of no interest. The noise

is assumed to be Gaussian additive white noise. A t test on the coefficient of the regression pertaining the stimulus function was performed. The maps were thresholded using an F statistics. A p value of 10^{-4} was chosen to display the results. All the preprocessing steps and the analysis were performed with AFNI [13].

B. Results

1) Phantom Tests: Table II summarizes the test results for the complete mechatronic device while scanning the phantom. The results show no significant difference between the image sequences with the running device and the baseline images.

The first experiment consisted of two reference image sequences with no device in the scanner room. The second experiment was performed with the interface in the scanner room at bore entrance, with both the master actuator of the hydrostatic transmission and the ultrasonic motor running.

TABLE II

Test results of the differences between the means of signal-to-noise ratio (SNR) and time domain standard deviation (t SD), estimated from images acquired under different experimental conditions: without the device and with the device running.

	Slice #5		Slice #10		Slice #20	
Experiment #	t SNR	z SD	t SNR	z SD	t SNR	z SD
1 Test between baseline images	0.45	0.23	0.41	0.02	−0.18	0.32
2 Device at bore entrance turned on	−0.15	1.86	−0.73	0.2	−0.91	0.25

2) Functional Study with a Subject: Fig. 5 shows the activation maps acquired during a finger tapping experiment. The left panel was obtained without any device in the MR room and the right panel with the device running as the subject was performing the finger tapping task. Both the maps show activation in the contralateral primary motor areas as well as in the supplementary motor areas. Minor activation is found in the primary sensory areas. Although preliminary and only qualitative, these results show that there is no significant difference in the neural maps activated by the tactile task with and without the device.

V. Conclusion

A 2DOF fMRI compatible mechatronic device that can be used for controlled presentation of dynamic tactile stimuli during functional imaging has been presented. The device can move a tactile stimuli below the finger of a subject, with the additional possibility of varying the orientation of the stimuli during the imaging. It will be used to explore the activation of specific areas of the brain in response to dynamic tactile stimuli.

The interface was designed using actuators and materials that were tested for MR compatibility in an early phase of the project. These tests, performed during the development phase of the mechatronic device, allowed the use of non-ferromagnetic metals, which present better mechanical properties than non-conducting polymers.

The development of the interface was completed with compatibility tests of the complete device. Tests were performed
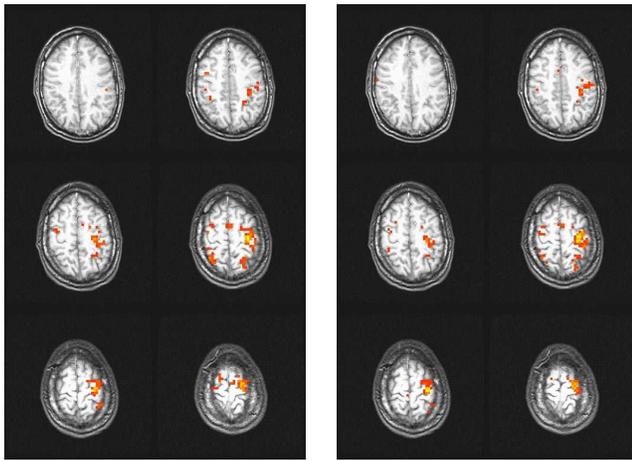
Fig. 5. Activation maps during a finger tapping experiment without the device (left) and with the device running (right). These are maps of the t test results on the regression coefficient of interest are thresholded with an F statistics ($p < 10^{-4}$).

both with a phantom and a subject, producing similar positive results. The detailed compatibility tests demonstrated that this device does not create image artifacts, and that it is MR safe and compatible in the experimental location.

The chosen design approach, based on systematic compatibility tests of materials and mechatronic components as well as tests of the complete device, is necessary to develop safe and efficient MR compatible robots.

REFERENCES

[1] J. Schenck, "The role of magnetic susceptibility in magnetic resonance imaging: MRI magnetic compatibility of the first and second kinds," *Medical Physics*, vol. 23, no. 6, pp. 815–850, June 1996.

[2] K. Ludeke, P. Roschmann, and R. Tischler, "Susceptibility artefacts in NMR imaging," *Magn Reson Imaging*, vol. 3, no. 4, pp. 329–343, 1985.

[3] Food and D. Administration, "A primer on medical device interactions with magnetic resonance imaging systems," *U.S. Department of Health and Human Services, http://www.fda.gov/cdrh/ode/primerf6.html*, 1997. [Online]. Available: http://www.fda.gov/cdrh/ode/primerf6.html

[4] R. Gassert, R. Moser, E. Burdet, and H. Bleuler, "An MRI/fMRI compatible robotic system with force-feedback for interaction with human motion," *IEEE/ASME Transactions on Mechatronics*, April 2006.

[5] D. Chapuis, R. Gassert, L. Sache, E. Burdet, and H. Bleuler, "Design of a simple MRI/fMRI compatible force/torque sensor," in *IEEE International Conference on Robotics and Intelligent Systems (IROS)*, 2004, pp. 2593–2599.

[6] "Shinsei Corporation Inc., USR60 series ultrasonic motor," *http://www.tky.3web.ne.jp/˜usmotor/English/html/*.

[7] J. Sijbers, A. den Dekker, J. Van Audekerke, M. Verhoye, and V. D. D, "Estimation of the noise in magnitude MR images," *Magn Reson Imaging*, vol. 16, no. 1, pp. 87–90, 1998.

[8] K. Thulborn, "Quality assurance in clinical and research echo planar functional MRI," in *Functional MRI*, B. P. Moonen, CTW, Ed. Springer-Verlag, 2000.

[9] R. Moser, R. Gassert, E. Burdet, L. Sache, H. Woodtli, J. Erni, W. Maeder, and H. Bleuler, "An MR compatible robot technology," in *Proc. IEEE International Conference on Robotics and Automation (ICRA)*, September 2003, pp. 670–675.

[10] G. Ganesh, R. Gassert, H. Bleuler, and E. Burdet, "Dynamics and control of an MRI compatible master-slave system with hydrostatic transmission," in *Proc. IEEE International Conference on Robotics and Automation (ICRA)*, 2004, pp. 1288–1294.

[11] J. Neter, W. Wasserman, and M. Kutner, *Applied Linear Statistical Models*, 2nd ed. Irwin, 1996.

[12] M. Cohen, "Parametric analysis of fMRI data analysis using linear system methods," *Neuroimage*, vol. 6, no. 2, pp. 93–103, 1997.

[13] R. Cox, "AFNI: software for analysis and visualization of functional magnetic resonance neuroimages," *Comput Biomed Res*, vol. 29, no. 3, pp. 162–173, 1996.